Journal of Mechatronics, Electrical Power, and Vehicular Technology 17 (2026) 15-27

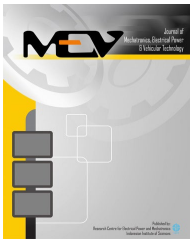

Journal of Mechatronics, Electrical Power, and Vehicular Technology

e-ISSN: 2088-6985
p-ISSN: 2087-3379

mev.brin.go.id

Design and implementation of hardware-in-the-loop simulation for haptic feedback control system validation in steer-by-wire

Noval Lilansa, Faisal Abdulrahman Budikasih, Fitria Suryatini, Nadya Zahra Putriutami *

Automation and Mechatronics Engineering, Bandung Polytechnic of Manufacturing
Jalan. Kanayakan 21, Dago, Bandung, Indonesia

Abstract

The advancement of steer-by-wire (SbW) technology in the modern automotive industry demands efficient and safe testing methods for complex control systems. Conventional validation on physical prototypes is often prohibitively expensive and high-risk, particularly in the initial development phases where control algorithms are still immature. To mitigate these challenges, hardware-in-the-loop (HIL) simulation provides a crucial intermediate step, enabling rapid, cost-effective, and safe iterative testing of control algorithms in a controlled environment. This research presents the design, implementation, and validation of a haptic feedback control system for an SbW application using a low-cost HIL platform. The developed architecture integrates a physical steering wheel plant with a real-time virtual model of the front wheels, controlled via an NI MyRIO and LabVIEW. The control system performance was analyzed by comparing proportional (P) and proportional-derivative (PD) controllers. The proportional controller was tuned using an empirical approach, while the proportional-derivative controller was designed analytically using the pole-zero cancellation method. The results demonstrated a clear trade-off with the proportional controller, which produced physical oscillations on the hardware. In contrast, the proportional-derivative controller successfully eliminated overshoot and damped all oscillations, which was physically validated as a stable and responsive haptic feedback. This research successfully demonstrates that the HIL platform can effectively validate and differentiate the physical performance of control architectures, confirming the superiority of the proportional-derivative controller for achieving a stable, high-fidelity haptic feedback system for SbW applications.

Keywords: steer-by-wire; hardware-in-the-loop (HIL); proportional control; haptic feedback; pole zero cancellation.

I. Introduction

With rapid advancements in the automotive sector, drive-by-wire technology has emerged as a crucial innovation. Its core concept involves replacing traditional mechanical components and linkages with electronic control systems and electromechanical actuators [1][2]. One of its primary implementations is steer-by-wire (SbW) technology, which revolutionizes vehicle steering systems by eliminating the direct mechanical connection between the steering wheel and wheels, replacing it with sensors, actuators, and an electronic control unit (ECU) [3][4][5]. The adoption of this technology shows a clear trend in the industry, with leading manufacturers such as Tesla, Toyota, and Lexus implementing SbW in their latest models.

An SbW system fundamentally consists of two main modules: the steering wheel module on the driver's side and the steering actuator module on the front wheels [6][7]. The steering wheel module is equipped with a sensor to detect the driver's input angle and a feedback motor to create a steering sensation (haptic feeling) [8].

* Corresponding Author. nadya.zahra02@gmail.com (N. Z. Putriutami)

https://doi.org/10.55981/j.mev.2026.1357

Received 17 December 2025; revised 23 January 2026; accepted 4 March 2026; available online 24 June 2026

How to Cite: N. Lilansa *et al.*, "Design and implementation of hardware-in-the-loop simulation for haptic feedback control system validation in steer-by-wire," *Journal of Mechatronics, Electrical Power, and Vehicular Technology*, vol. 17, no. 1, pp. 15-27, July, 2026.

The signal from this sensor was processed by the ECU, which then sent a command to the actuator motor to turn the front wheels. Simultaneously, the ECU calculates the appropriate road reaction force and commands the feedback motor to generate a counter-torque on the steering wheel, thus providing a natural driving experience [8].

One of the greatest challenges in SbW development is the design of a haptic feedback control system capable of providing a realistic and safe steering sensation for the driver [9]. Direct validation of a full-vehicle prototype in development is extremely expensive, time-consuming, and high-risk, especially in the early development stages where control algorithms are still immature. System failure can lead to costly hardware damage or compromise safety. Therefore, a testing method that allows iterative validation in a safe and controlled environment is required.

To address these challenges, the hardware-in-the-loop (HIL) simulation method offers a highly effective solution. HIL is a development practice that integrates a physical hardware component into a closed-loop simulation with other system components that are virtually modelled [10]. This approach substitutes for expensive and time-consuming physical testing, allowing a controller to be rigorously validated across thousands of potential scenarios without associated costs and risks [10]. The simulation finds application in different areas, such as wind energy converters [11] and systems [12], unmanned aerial vehicles (UAVs) [13], [14], automation [15], and automotive fields [16].

In addition to sophisticated HIL simulators, such as those provided by Typhoon, OPAL-RT, dSPACE, Plexim's RT Box, Speedgoat, and NI, low-cost simulators are also available for simulating less-complex systems in many applications. Low-cost HIL simulations have been proposed by many researchers for less-complex systems in the fields of control, energy, and automation. Romdlony *et al.* [17] developed a low-cost HIL simulation dedicated to instructional media in control systems. In the simulation, Arduino was applied as the main controller, and a mathematical model of the DC motor, which served as the plant, was implemented in LabVIEW. Data acquisition of type NI USB-6008 was also included to communicate between the controller and the model. The results demonstrate the efficacy of the HIL simulation.

Goubej *et. al.* [18] proposed another low-cost HIL simulator intended for a control-engineering course. Two Raspberry Pis were used in the proposed simulator: one Raspberry Pi was used as the controller, and the other simulated a quarter-car suspension through a mathematical model. The simulator and controller were connected via a Monarco HAT. A survey of the proposed HIL was conducted, which showed a clearly positive response. In the field of control engineering, Tejado *et al.* [19] presented a low-cost HIL application for mobile robots to support learning in automatic control and robotics. The robot simulator was built using the MATLAB®/Simulink® environment, and Arduino was implemented as the controller. Communication between the controller and simulator was performed via TCP/IP. The developed HIL demonstrated that some possible control courseware could be implemented. Martinez-Armero *et al.* [20] presented another low-cost HIL simulation based on Arduino. The simulation proposed two DUE Arduinos, with one Arduino acting as the controller and the other used to simulate the plant. The HIL simulation was tested by applying three multivariable dynamic systems: an RLC system, a twin-rotor MIMO system, and a microgrid. The proposed low-cost HIL simulation successfully performed a detailed controller analysis.

Jiang *et al.* [21] proposed a low-cost hardware-in-the-loop on-chip platform for teaching and designing dynamic systems, particularly for digital power converters. In the platform, a dual-core digital signal controller (DSC) was implemented, with one core serving as the simulation engine and the other as the control engine. The proposed HIL successfully demonstrated the buck and boost topology of the power converter and a dual-tank process control system. This demonstrates the ease of application in engineering teaching. Furthermore, the on-chip platform succeeded in fast prototyping, which was conducted during the development phase of product design.

This study proposes an alternative low-cost HIL system for the design, implementation, and performance analysis of a haptic feedback control system for SbW. The HIL system comprises the NI MyRIO-1900 serving as the real-time data acquisition and control unit, and LabVIEW software was used as the development environment for simulating the virtual model and designing the human-machine interface (HMI). The main contributions of this research are as follows: (1) the design and implementation of a low-cost HIL platform, (2) the determination of an effective tuning method for the designed physical plant by applying the pole-zero cancellation method, and (3) analysis of the oscillation dynamics caused by interactions within the haptic feedback loop.

II. Materials and Methods

Figure 1 depicts the research methodology for the design and implementation of HIL simulation for haptic feedback control system validation in SbW, which adopts a systematic and iterative workflow. The process begins with a comprehensive definition of the system requirements, which serves as the foundation for the system modelling and high-level architectural system design stages. This is then broken down into a detailed design at the domain-specific design level, encompassing the mechanical, electrical, and informatics domains. Before physical implementation, a crucial validation step is performed on the virtual model via simulation (validation model system), and if the model fails, the workflow returns to the modelling stage for refinement. Once the model is validated, the research proceeds to system integration, in which the hardware and software components are combined. The integrated system then underwent a final testing against the initial requirements. A failure at this stage triggers a fundamental re-evaluation, while success signifies that the system has been validated, and the research objectives have been achieved. This methodology ensures a structured approach with dual validation cycles (virtual and physical) to minimize risk and ensure the reliability of the final system. Following this methodology, the research is structured into several key stages, which are detailed in the subsequent sub-chapters.

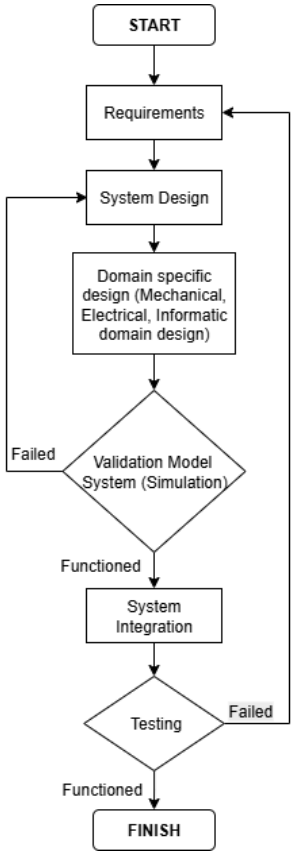

Figure 1. Flowchart of the research methodology.

A. System design

Figure 2 illustrates the design of the physical plant employed in this study, which consists of a steering simulator. This plant serves as the primary interface where the system receives angular rotation input from the user and acts as an actuator to provide haptic feedback. The simulator was designed with main dimensions of 300 mm × 120 mm and a steering wheel diameter of 303.6 mm to represent realistic driver interaction. The transmission of rotation from the shaft to the sensor and actuator uses a timing belt and pulley system to ensure a precise and reliable motion transfer.

Within the developed HIL architecture, a physical steering simulator was integrated with a mathematical model of the front wheel. The integration between the physical world (simulator) and the virtual world (mathematical model) is bridged by the NI MyRIO controller, with the entire system logic and model being implemented in the LabVIEW software.

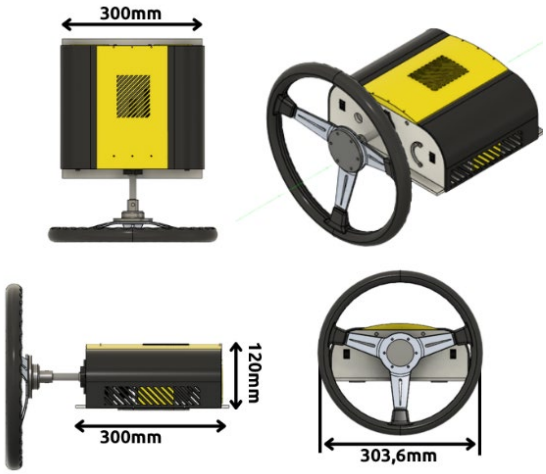

Figure 2. CAD design of the steering simulator's physical plant.

B. Mechanical domain design

The mechanical design in this study is divided into two main subsystems, representing the physical architecture of the SbW system: the steering wheel module (Figure 3), which serves as the driver interface, and the wheel actuation module (Figure 4), which functions as the command executor.

To analyze and control the dynamics of these mechanical subsystems, a mathematical model was developed. This model defines the dynamics of both the steering wheel and front-wheel execution modules. The steering wheel's behavior is described by a second-order differential equation that balances the driver's input torque (T_h) and haptic feedback torque (T_f) against the wheel's own inertial (J_h) and damping (B_h) properties. The equation for steering wheel angle are equation (1) and equation (2) [22].

$$J_h\,\ddot{\theta}_h + B_h\,\dot{\theta}_h + C_h\theta_h = T_h - T_f \quad (1)$$

$$\ddot{\theta}_h = \frac{1}{J_h}\left(B_h\,\dot{\theta}_h - C_h\theta_h + T_h - T_f\right) \quad (2)$$

Similarly, the front-wheel steering execution module is modelled to describe how the actuator torque (T_{eq}) overcomes the equivalent inertia (J_{eq}), damping (B_{eq}), and friction ($F_S sign(\dot{\theta}_f)$) of the wheel assembly. A critical component of this model is the self-aligning torque (T_e), which represents the natural force from the tire-road interaction that tends to straighten the wheel, and is calculated based on various vehicle dynamic parameters. The equation for the steering execution module are equation (3) and equation (4) [22].

$$J_{eq}\,\ddot{\theta}_f + B_{eq}\,\dot{\theta}_f + F_S sign\left(\dot{\theta}_f\right) + T_e = T_{eq} \quad (3)$$

$$\ddot{\theta}_f = \frac{1}{J_{eq}}\left(-B_{eq}\,\dot{\theta}_f - F_S sign\left(\dot{\theta}_f\right) T_e - T_{eq}\right. \quad (4)$$

The self-aligning torque equations in both equation (3) and equation (4) can be described as equation (5) [22].

$$T_e = T_e(\theta_f) = -C_f(l_c + l_p)\left(\beta + \frac{\gamma l_f}{v} - \theta_f\right) \quad (5)$$

Table 1 and Table 2 list the parameters used in the simulation according to equation (3), equation (4), and equation (5), respectively. In equation (4), E_{Tot} is the total energy consumed for each communication event between nodes. This model enables the evaluation of energy efficiency based on data transmission and reception patterns within the network. Moreover, determining the distance threshold d_0 provides crucial insights for optimizing routing protocols, ultimately extending the operational lifespan of wireless sensor networks.

C. Electrical domain design

Figure 5 depicts the electrical design, which covers the integration of all electronic components. An incremental rotary encoder (1000 PPR) was connected to the digital inputs of the NI MyRIO-1900 for data

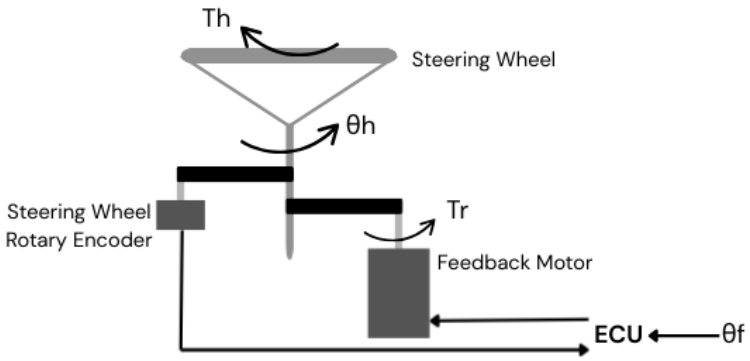

Figure 3. Schematic diagram of the steering wheel module.

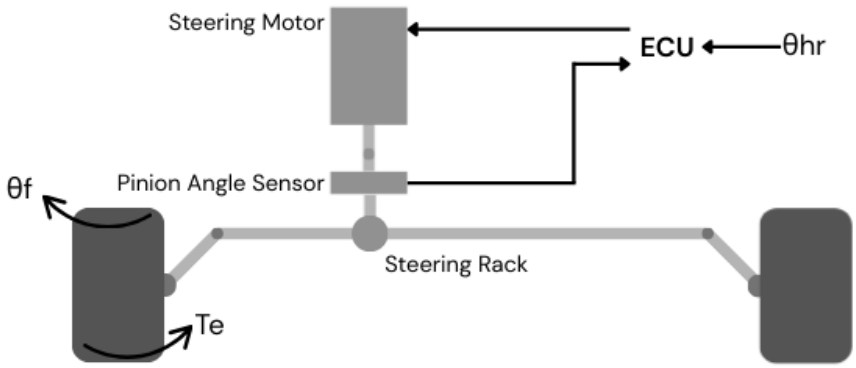

Figure 4. Schematic diagram of the front wheel actuation module.

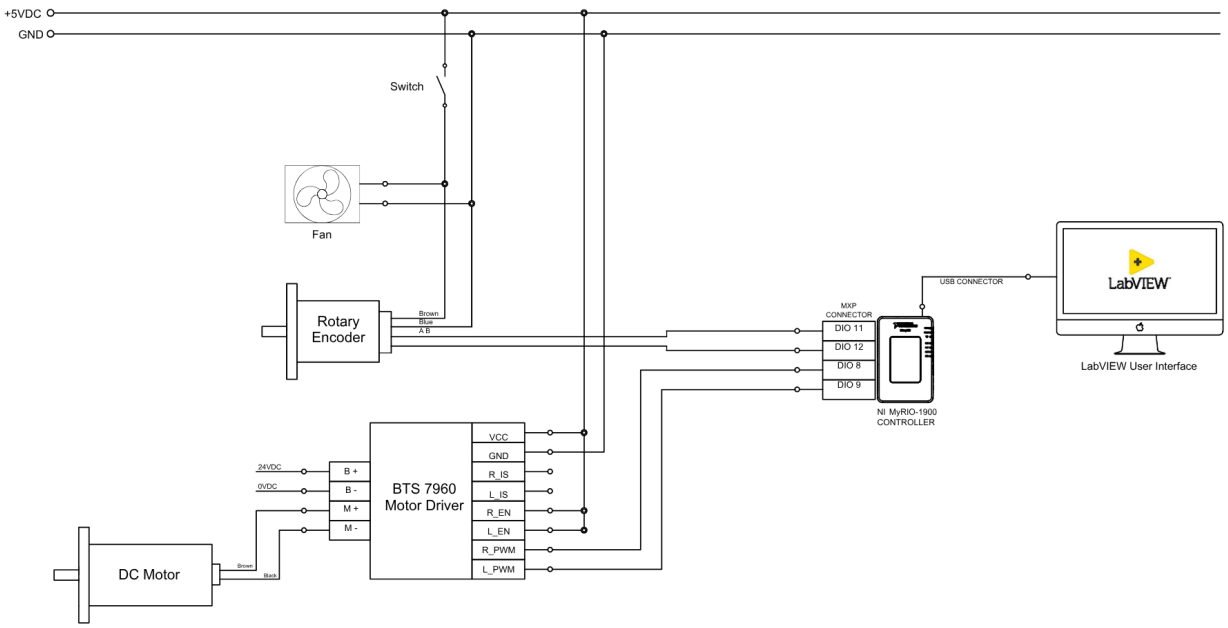

Figure 5. Electrical schematic diagram of the system.

acquisition of the angular position. A 12 V DC motor serving as the haptic feedback actuator was controlled by a BTS7960 H-Bridge motor driver that received a PWM signal from NI MyRIO. The entire system is powered by a 5 VDC supply for logic and a 12 VDC supply for the motor, with NI MyRIO-1900 acting as the central data acquisition and control hub.

Table 1.
SbW system parameters for simulation.

Parameter	Value	Unit
J_h	0.038	$kg.m^2$
B_h	0.15	Nms/rad
C_h	0.2	Nm/rad
J_{fw}	2.6	$kg.m^2$
B_{fw}	12	Nms/rad
J_{sm}	0.006	$kg.m^2$
B_{sm}	0.01	Nms/rad
F_s	2.68	Nm
N_2/N_1	3	unitless
r	6	unitless
N	18	unitless
r_q	8.5	unitless

Table 2.
SbW system parameters for simulation.

Parameter	Value	Unit
I_z	1300	$kg.m^2$
l_c	0.016	m
l_p	0.023	m
l_f	1.2	m
l_r	1.05	m
C_f	12000	N/rad
C_r	12000	N/rad
v	126	km/h

D. Informatics domain design

Figure 6 shows a block diagram of the integrated dual-loop control architecture for the SbW system. The process begins with the driver turning the steering wheel, which is regarded as the disturbance torque to the steering wheel closed-loop. The disturbance causes a change in the actual steering wheel position (θ_h), which, in comparison with the actual front wheel position (θ_f), results in an error in the closed-loop. The PID controller of the feedback motor produces a control signal to the feedback DC motor to generate a counter torque (T_R) so that the driver can feel the change in the reaction torque while holding the steering wheel. This creates a haptic feedback sensation that is felt directly by the driver. In this study, the steering wheel system was the physical hardware under test. Simultaneously, the actual steering-wheel position (θ_h) serves as the input for the second control loop, where this signal is scaled by the steering ratio $(1/N)$ to serve as the setpoint for the front wheels. This setpoint is then compared with the actual front-wheel position (θ_f), and the error resulting from the comparison is processed by the PID Controller of the front wheel. The controller then issues a command to the front-wheel system, which is represented as a mathematical model within the HIL simulation, to move the wheels until the target angle is reached with precision. Thus, this HIL architecture effectively separates the driver's physical interaction with the hardware plant (haptic loop) from the wheel actuation

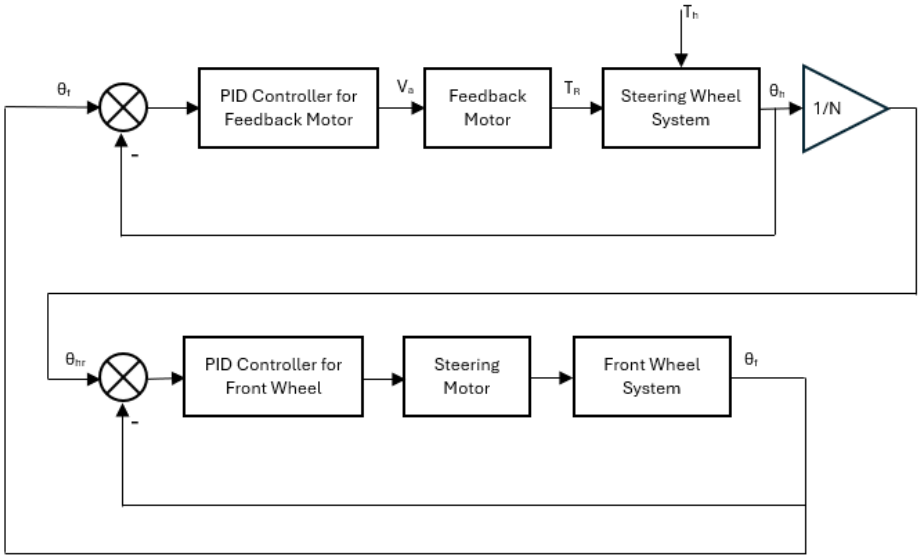

Figure 6. Block diagram of the steer-by-wire system architecture.

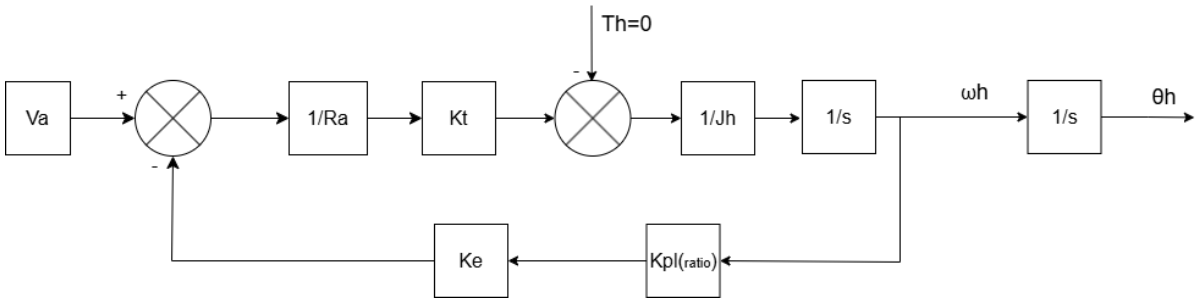

Figure 7. Block diagram of the DC motor dynamic model.

that runs in the virtual domain (position control loop), where both are sequentially connected to achieve a responsive and controlled driving experience.

The control system domain encompasses the mathematical modelling, analysis, and design of the control strategy for the feedback motor plant. The control system design in this study aims to regulate the position of the haptic DC motor (θ_h) to follow the input voltage reference (V_a) of the feedback DC motor, as depicted in Figure 6. The design aims to obtain an accurate and fast response to position. The former can be achieved with a zero steady-state error, whereas the last with cancelling dominant poles exists in the control system. The first step is to analyze the mathematical model of the position of the DC motor, as illustrated in the block diagram depicted in Figure 7. From the block diagram, the closed-loop transfer function of the motor (G_h) can be expressed as equation (6).

$$\frac{\theta_h(s)}{V_a(s)} = G_h(s) = \frac{K_t}{s(R_a.J_h.s+K_t.K_e.K_{pl})} \quad (6)$$

the parameters used in this study are stated, R_a is 8 Ohm, K_t is 0.01 Nm/A, J_h is 0.038 kgm^2, K_e is 0.01, K_{pl} is 5.

The resulting transfer function in equation (6) is then analyzed to determine the PID configuration for the steering wheel system. According to equation (6), the transfer function is a second-order, type 1 system. Because of the type 1 system, the integral term of the PID controller is therefore not required to achieve zero steady-state error for the unit step input [23]. Consequently, only two controller configurations are required: A proportional (P) controller and a proportional plus derivative (PD) controller. For the P controller, an empirical tuning approach was applied. This method involves systematically varying the gain K_p of the controller while observing and evaluating the system's response to a step input based on performance metrics such as overshoot and settling time to find the value that provides the best compromise. Meanwhile, for the PD controller, a different analytical design method was used, namely pole-zero cancellation. This method strategically uses the zero introduced by the PD controller to cancel out one of the dominant poles of the plant. By using these two approaches, this research can comprehensively compare the effectiveness of both control strategies.

With a general controller $G_c(s)$, the closed-loop transfer function $G_f(s)$ of the steering wheel can be expressed as equation (7).

$$G_f(s) = \frac{G_c(s).G_h(s)}{1+G_c(s).G_h(s)} \quad (7)$$

where G_c represents the transfer function of the controller, and Gh is the transfer function of the feedback DC motor. An empirical tuning approach was applied to the P controller. This method involves systematically varying the gain K_p and evaluating the step response of the system based on performance metrics to find the best compromise. With $G_c(s) = K_p$, the closed-loop transfer function becomes equation (8).

$$G_f(s) = \frac{\theta_h(s)}{\theta_f(s)} = \frac{K_p/(K_e\,K_{pl}\,\tau_h)}{s^2+(1/\tau_h)\,s+K_p/(K_e\,K_{pl}\,\tau_h)} \quad (8)$$

where τ_h represents the time constant of the feedback DC motor and can be expressed as equation (9).

$$\tau_h = \frac{R_a.J_h}{K_t.K_e.K_{pl}} \quad (9)$$

For the PD controller design, an analytical method of pole-zero cancellation was implemented. This approach begins with the use of a more realistic form of the PD controller with the transfer function as equation (10) [23].

$$\mathrm{G_c(s)} = K_p\,.\frac{1+s(T_v+T_c)}{1+sT_c} \quad (10)$$

This form was selected because it includes a low-pass filter $(1 + sT_c)$ to mitigate noise amplification, which is a practical issue with ideal PD controllers. According to [23], T_v was chosen to be 3 - 50 times higher than T_c. The primary objective of this method is to strategically place the controller's zero, located at $s = \frac{-1}{(T_v+T_c)}$, to cancel out one of the dominant poles existing in the motor plant, which can cause a slow response. Concerning (10), the open-loop transfer function (G_o) of the steering wheel loop can be written as equation (11).

$$G_o(s) = \frac{1+s(T_v+T_c)}{1+sT_c}.\frac{K_p}{K_e.K_{pl}}.\frac{1}{(\tau_h\,s+1)s} \quad (11)$$

Applying pole-zero cancellation to equation (11) results in the following equation (12).

$$T_v + T_c = \tau_h \quad (12)$$

equation (11) and equation (12) give rise to the following closed-loop transfer function as equation (13).

$$G_f(s) = \frac{K_p/(K_e\,K_{pl}\,T_c)}{s^2+(1/T_c)\,s+K_p/(K_e\,K_{pl}\,T_c)} \quad (13)$$

From equation (8) and equation (13), it can be deduced that the proportional term (K_p) in both the Pand PD controllers affects the speed of the system response, as shown in the numerator and the coefficient of s^0 in the denominator of both equations. The higher the value of K_p, the faster the response. On the other hand, applying the PD controller with pole-zero cancellation removes the effect of the feedback DC motor time constant (τ_h).

E. Simulation

Figure 8 presents a model-in-the-loop (MIL) simulation for a steer-by-wire system implemented in the LabVIEW program and validated using the Runge-Kutta method. The control architecture clearly shows two interconnected primary loops. The main control loop is responsible for driving the front wheel (Front Wheel.vi) to match the position reference from the steering wheel (SUB-Steering Wheel.vi). The front-wheel control loop utilizes a proportional-derivative (PD) controller with tuned gain values ($K_p = 450$ and $K_d = 1.4$) to generate the front-wheel motor torque signal. Furthermore, the vehicle was assumed to move on a dry asphalt road and its velocity was set to

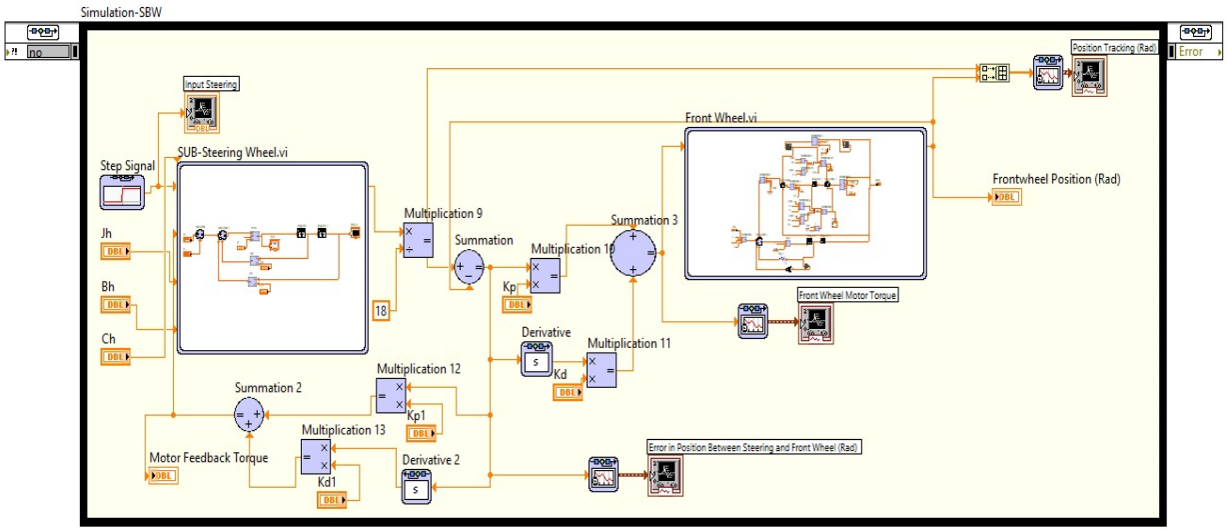

Figure 8. Block diagram of the model-in-the-loop (MIL) simulation implementation in LabVIEW.

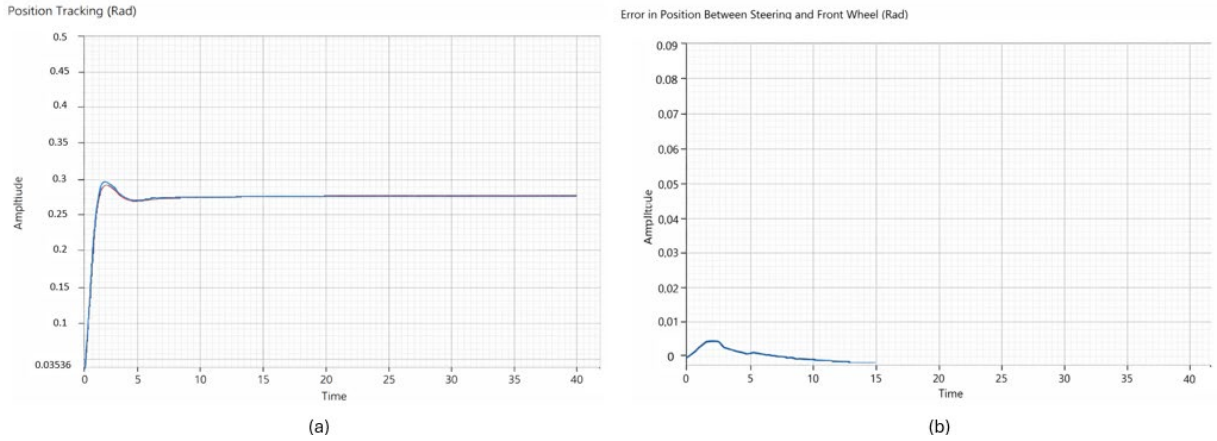

Figure 9. System response graphs to a step input: (a) position tracking and (b) position error.

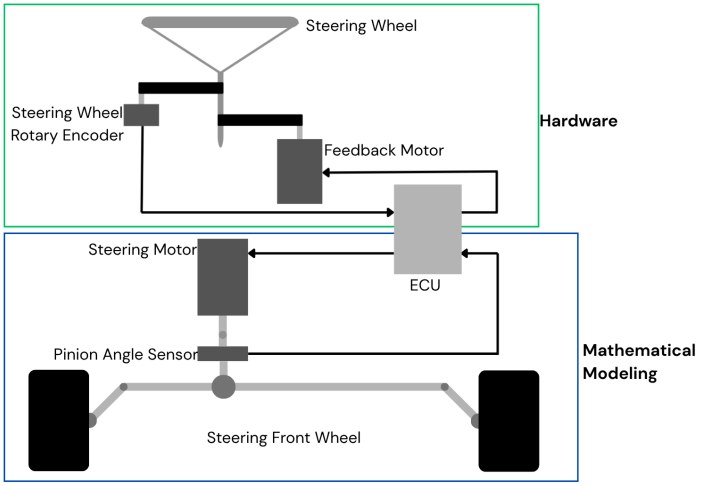

Figure 10. Separation of physical (hardware) and virtual (mathematical modeling) components.

126 km/h. The error for this controller was calculated from the difference between the reference position of the steering wheel and the actual front-wheel position. In addition, a haptic feedback control loop, also modeled as a PD controller (K_{p1}, K_{d1}), was presented. This loop calculates the motor feedback torque based on the same position error, which is then fed back into the steering wheel model to simulate the forces felt by the driver. This structure accurately represents the logic of a steer-by-wire system, where controlling the wheel position and providing force feedback to the driver are the two main objectives.

An analysis of the 40-second simulation results, as shown in Figure 9, demonstrates excellent control system performance and successfully validates the transfer function models. In the "Position Tracking (Rad)" graph, it is evident that the actual front wheel position (red line) is able to follow the step reference signal from the steering wheel (blue line) of approximately 0.28 radians with high responsiveness. The system exhibited fast transient response characteristics, featuring a short rise time and reaching the target in less than 2 s. A very slight overshoot was observed, indicating that the system was well-damped and did not oscillate excessively before finally reaching a steady state in approximately 5 s. This is further confirmed by the "error in position between steering and front wheel (rad)" graph, where the initial error of ~0.09 radians is effectively attenuated by the controller, permanently approaching zero after the 5-second mark. The absence of a steady-state error proves that the designed PD controller is highly effective for achieving precise position tracking. Overall, these simulation results strongly confirm that the developed mathematical models and tuned controller parameters can produce a control system that is fast, stable, and accurate, thereby meeting the expected design specifications.

F. System integration

Integration is performed by combining the hardware of the steering wheel and the mathematical model of the front wheel with the structure shown in Figure 10. The hardware of the steering wheel is shown in Figure 11. It consists of an on-off switch (1), a fan for cooling (2), a rotary encoder for measuring the angular position of the steering shaft (3), a DC motor for a feedback motor (4), a motor driver of type BTS 7960 for

a feedback motor driver (5), and NI myRIO – 1900 (6). The NI myRIO is tasked with acquiring sensory data (such as the rotational angle) from the hardware while simultaneously sending actuation signals (force feedback) back to the hardware.

Figure 12 shows the HIL architecture implemented in this study. The developed HIL architecture consists of several key components that operate in an integrated manner:

a. *Host computer*: A PC running LabVIEW software, serving as the development environment, monitoring station, and human-machine interface.
b. *Real-time target and I/O interface* (ECU): This role was fulfilled by NI MyRIO-1900. This device is responsible for executing the control logic in real time and acts as a bridge between the digital domain (simulation) and physical domain (plant) through its analog and digital input/output (I/O) channels.
c. *Hardware under test (HUT)*/physical plant: This real hardware component being tested is a steering column assembly equipped with a DC motor as a haptic feedback actuator and a rotary encoder as an angular position sensor (steering simulator).
d. *Simulation model* (virtual model): A mathematical model running on the host computer (LabVIEW). This model simulates the dynamics of the vehicle's front wheels, which do not exist physically. The model includes the implementation of a 1:18 steering ratio and the calculation of road reaction forces (self-aligning torque), which form the basis of the haptic feedback signal.

The control logic and data processing on the MyRIO were programmed using the LabVIEW platform, which acts as a software development environment. Furthermore, the LabVIEW application on the controller communicates with a user interface running on a laptop. This interface serves as an HMI, allowing the operator to monitor telemetry data in real time, modify simulation parameters, and issue high-level commands to the system. The interaction between the above components forms a closed loop: the position signal from the HUT is read by the real-time target, which is then fed into the simulation model on the host computer. The output from the model (haptic signal) is sent back through the real-time target to drive the actuator on the HUT, thus closing the loop. Overall, this architecture creates a robust ecosystem for mechatronic system validation, in which a physical

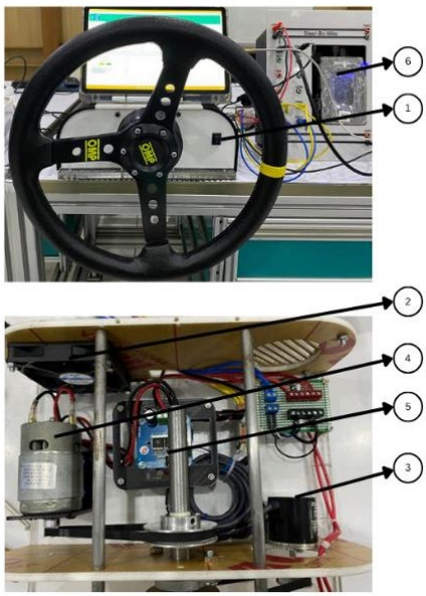

Figure 11. Steering wheel hardware.

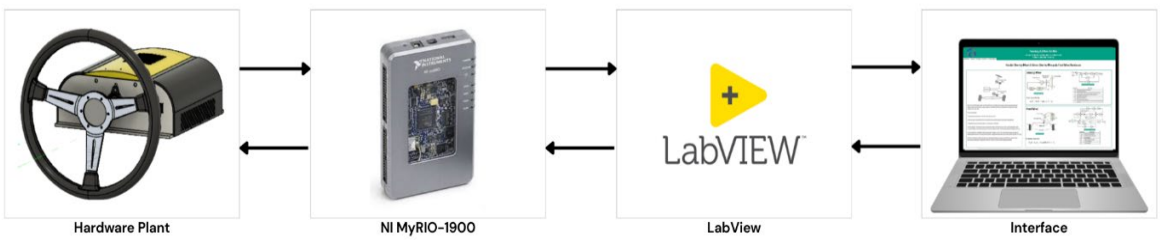

Figure 12. The Hardware-in-the-Loop (HIL) system architecture diagram.

component is tested through its interaction with a precisely controlled virtual environment.

III. Results and Discussions

A. Proportional controller tuning result

Table 3 presents the quantitative results of the tuning process of a P controller, where the proportional gain (K_p) varies from 1 to 9. The test was conducted by applying a 90-degree step reference input to the steering wheel system. The system performance was evaluated based on five transient and steady-state response metrics: peak time (T_p), settling time (T_s), rise time (T_r), and maximum overshoot (M_p). Several clear trends are observed in the presented data. In general, an increase in the Kp value tends to accelerate the system response, as indicated by the decreasing values of the rise time (T_r) and peak time (T_p). This aligns with control theory, where a higher gain produces a larger and faster control action. However, this speed results in a trade-off in stability. Mp fluctuates, but remains at an acceptable level (below 7 %) for Kp values from 1 to 8. However, there was a very significant spike in the overshoot to 14.4 % when Kp was increased to 9. This spike indicates that the system becomes highly underdamped and approaches the stability limit. This phenomenon also affects Ts, where the lowest value is achieved at $K_p = 8$ (1721 μs), but then drastically worsens at $K_p = 9$ (2365 μs) due to excessive oscillation. For all test cases, the steady-state error (E_{ss}) was consistently zero, which validates that the controller can eliminate the steady-state error for the given setpoint.

B. Proportional-derivative controller tuning results

Table 4 presents the experimental results from the tuning process of a PD controller. Specifically, this test was conducted by keeping the derivative gain (K_d) constant at 0.608, while the proportional gain (K_p) was varied from 1 to 8. As in the previous test, the system was evaluated using a 90-degree step reference input on the steering wheel, and its performance was measured based on standard response metrics.

Based on the data, a K_p value of four (the highlighted row) was selected as the optimal proportional gain to be combined with $K_d = 0.608$. This choice was based on the objective of obtaining the fastest possible response with zero overshoot. Although the lower gains (K_p = 1,2) are slightly faster, they still exhibit a small overshoot. Starting from K_p = 3, the system successfully achieved an overshoot of 0.0 %. Among all the zero-overshoot options (K_p = 3, 4, 7, 8), K_p = 4 provided the fastest settling time (3968 μs). Increasing K_p further slows down the system response drastically without providing any improvement to the

Table 3.
P controller tuning results.

Proportional gain	Peak time (T_p)	Settling time (T_s)	Rise time (T_r)	Max overshoot (M_p)
1	1676 μs	2052 μs	1031 μs	6.4 %
2	1592 μs	2508 μs	931 μs	6.6 %
3	1531 μs	2352 μs	969 μs	4.9 %
4	1562 μs	2487 μs	988 μs	4.8 %
5	1595 μs	1915 μs	907 μs	5.2 %
6	1467 μs	1965 μs	903 μs	4.6 %
7	1363 μs	1935 μs	875 μs	5.7 %
8	1254 μs	1721 μs	849 μs	4.2 %
9	1412 μs	2365 μs	708 μs	14.4 %

Table 4.
PD controller tuning results.

Proportional gain	Peak time (T_p)	Settling time (T_s)	Rise time (T_r)	Max overshoot (M_p)
1	3109 μs	3273 μs	2301 μs	0.8 %
2	3430 μs	3430 μs	2133 μs	0.6 %
3	6450 μs	6158 μs	2133 μs	0.0 %
4	3968 μs	3968 μs	2750 μs	0.0 %
5	3692 μs	3692 μs	2454 μs	0.2 %
6	3513 μs	3513 μs	2397 μs	0.2 %
7	4501 μs	4501 μs	2929 μs	0.0 %
8	11760 μs	11760 μs	10099 μs	0.0 %

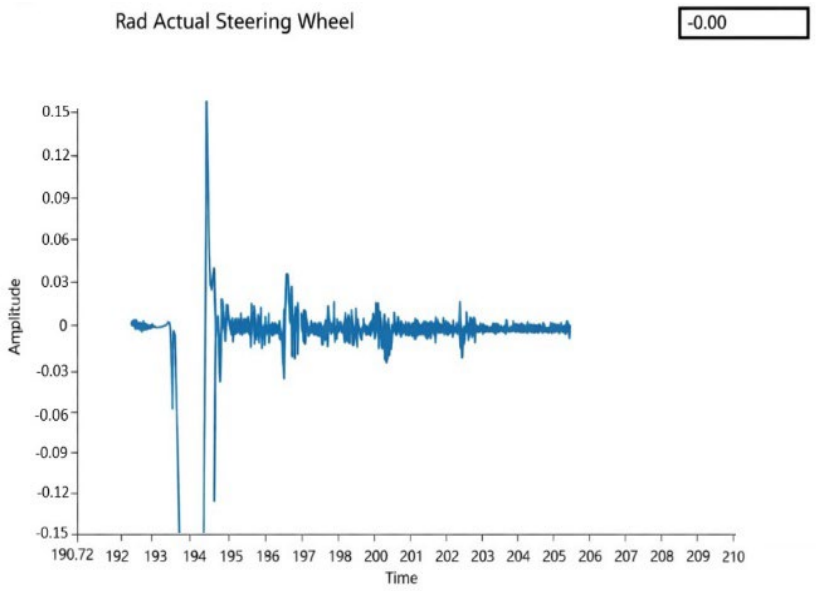

Figure 13. Actual steering wheel position response with the P controller.

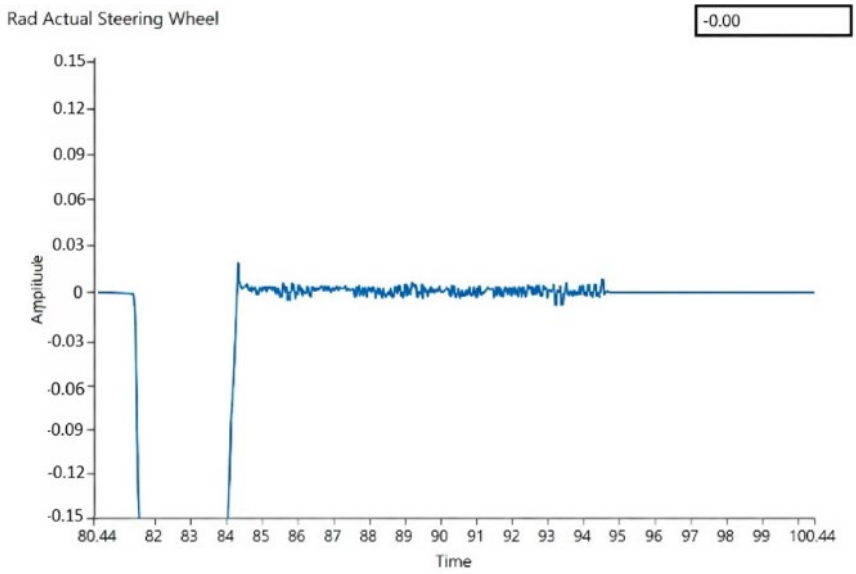

Figure 14. Actual steering wheel position response with the PD controller.

overshoot. Therefore, $K_p = 4$ represents the best balance between speed and achievement of the zero-overshoot target.

C. Analysis haptic feedback loop dynamics

The critical importance of the drastic difference between these two responses is apparent within the context of the HIL simulation, where the physical haptic feedback is generated from the mathematical model in equation (3), equation (4), and equation (5). It should be noted that the torque felt at the steering wheel is not a direct measurement but the result of a manipulated signal calculated by the controller logic of the front wheel. This mathematical signal is then sent to drive the motor on the actual steering wheel hardware. In the case of the P controller, an inherently oscillatory signal was generated owing to the absence of damping, as shown in Figure 13. Consequently, the hardware is commanded by this signal to reproduce unwanted reciprocating movements, which are then perceived by the user as chattering and unstable jolts, as validated by the first graph. Conversely, with the PD controller, the calculated signal is rendered non-oscillatory and stable through the damping action of the derivative component, as depicted in Figure 14. When this stabilized signal is sent to the motor, firm and controlled force feedback is executed by the hardware, as demonstrated in the second graph. This distinction is therefore crucial, as it provides a tangible validation of how the stability characteristics of a controller designed in the virtual domain are directly translated into the quality of the physical interaction experienced on the hardware-in-the-loop.

IV. Conclusion

This research was conducted to address the primary challenges in the development of steer-by-wire (SbW) systems by validating control systems for real vehicle prototypes. By successfully designing and implementing a low-cost hardware-in-the-loop (HIL) platform, this study provides an effective solution to these challenges. The developed platform created a safe, controlled, and cost-effective environment for the iterative design and testing of the haptic feedback control system, thereby directly addressing the need for a more efficient validation methodology. Furthermore, the HIL platform was used to solve the specific challenge of designing a realistic and safe haptic feedback mechanism. Through a systematic comparison, this study provides a definitive answer regarding the appropriate control architecture. The results clearly demonstrated that, despite being empirically tuned for optimal performance, a simple proportional (P) controller produced an unstable physical response with undesirable oscillations and chattering. In contrast, the proportional-derivative (PD) controller, designed analytically using pole-zero cancellation, was validated to produce a stable, smooth, and precisely controlled haptic response on physical hardware. This finding confirms that the inclusion of derivative (damping) action is crucial for recreating a high-quality steering feel. In summary, the main contributions of this work are the successful implementation of a low-cost HIL platform for SbW validation, a comparative analysis of empirical and analytical tuning methods, and a clear validation of the superiority of the PD controller in eliminating unwanted oscillation dynamics in the haptic loop. For future development, this validated platform can be used to test more advanced control algorithms and to incorporate more complex virtual models, such as varying road friction or tire properties, to further enhance the realism of haptic feedback.

Acknowledgements

The authors would like to express their sincere gratitude to Politeknik Manufaktur Bandung for the financial support, facilities, and institutional resources provided for this research. The authors also gratefully acknowledge the support of the Department of Automation and Mechatronics Engineering in facilitating the implementation of this study.

Declarations

Author contribution

Noval Lilansa: Conceptualization, Methodology, Supervision, Formal analysis, Writing - Review & Editing. **Faisal Abdulrahman Budikasih**: Investigation, Software, Validation, Data Curation, Writing - Original Draft, Visualization. **Fitria Suryatini**: Methodology, Resources, Validation, Writing - Review & Editing. **Nadya Zahra Putriutami**: Formal analysis, Supervision, Project administration, Writing – Review & Editing, Correspondence handling.

Funding statement

This research was supported by Politeknik Manufaktur Bandung through institutional research support, facilities, and laboratory resources.

Competing interest

The authors declare that they have no known competing financial interests or personal relationships that could have appeared to influence the work reported in this paper.

The use of AI or AI-assisted technologies

During the preparation of this work, the authors used ChatGPT by OpenAI to assist in improving grammar and language clarity. After using this tool, the authors reviewed and edited the content as needed and take full responsibility for the content of the publication.

Additional information

Reprints and permission: information is available at https://mev.brin.go.id/.

Publisher's Note: National Research and Innovation Agency (BRIN) remains neutral with regard to jurisdictional claims in published maps and institutional affiliations.

References

[1] S. S. Husain, M. Q. Kadhim, A. Sh. M. Al-Obaidi, A. F. Hasan, A. J. Humaidi, and D. N. Al Husaeni, "Design of robust control for vehicle steer-by-wire system," *Indones. J. Sci. Technol.*, vol. 8, no. 2, pp. 197–216, Dec. 2022.

[2] S. Achyuthan and N. K. Prakash, "Modelling of a steer-by-wire system with force feedback and active steering," in 2017 *International Conference on Intelligent Computing and Control Systems (ICICCS), Madurai: IEEE*, Jun. 2017.

[3] S. Zou, W. Zhao, C. Wang, W. Liang, and F. Chen, "Tracking and synchronization control strategy of vehicle dual-motor steer-by-wire system via active disturbance rejection control," *IEEEASME Trans. Mechatron.*, vol. 28, no. 1, pp. 92–103, Feb. 2023.

[4] M. Z. M. Tumari, M. S. Saealal, W. N. A. Rashid, S. Saat, and A. M. Nasir, "The vehicle steer by wire control system by implementing PID controller," *Journal of*

Telecommunication, Electronic and Computer Engineering (JTEC), vol. 9, no. 3-2, pp. 43-47, Oct. 2017.

[5] M. Zaidi Mohd Tumari *et al.*, "The control schemes of vehicle steer by wire system by using Fuzzy Logic and PID controller," *Res. J. Appl. Sci.,* vol. 13, no. 2, pp. 137–145, Nov. 2019.

[6] H. Yin, Z. Wang, J. Liu, and P. Liu, "Steer-by-wire control algorithm using a dual-layer closed-loop models," *Sci Rep*, vol. 14, no. 28536, 2024.

[7] M. A. Azizul, F. Ahmad, J. Karjanto, M. H. Che Hasan and S. Sulaiman, "Modelling, simulation and testing of steer-by-wire system with variable steering ratio control strategy in 14-DOF full vehicle model," *Int. J. Automot. Mech. Eng.*, vol. 21, no. 4, pp. 11784–11808, Nov. 2024.

[8] C. Su, H. Li, B. Qiao, and X. Wu, "Personalized steering feel design for steer-by-wire systems based on the rack force estimation," *Int. J Automot. Technol.*, vol. 24, pp. 1151 - 1161, 2023.

[9] T. Chugh, F. Bruzelius, M. Klomp, and B. Shyrokau, "Design of Haptic feedback control for steer-by-wire," in *Proceedings of 2018 21st International Conference on Intelligent Transportation System, Maui: IEEE*, Nov., pp. 1737-1744, 2018.

[10] F. Mihalič, M. Truntič, and A. Hren, "Hardware-in-the-loop simulations: A historical overview of engineering challenges," *Electronics*, vol. 11, no. 15, pp. 2462, Aug. 2022.

[11] M. Neshati, H. Zhang, P. Thomas, M. Heller, A. Zuga, and J. Wenske, "Evaluation of a hardware-in-the-loop test setup using mechanical measurements with a DFIG wind turbine nacelle," *J. Phys. Conf. Ser.*, vol. 2265, no. 2, p. 022105, May 2022.

[12] A. Gambier, "Real-time control and hardware-in-the-loop simulation for educational purposes of wind energy systems," *IFAC-PapersOnLine*, vol. 53, issue 2, 2020.

[13] A. R. Harits Martawireja, N. Lilansa, Y. Rajib, and Y. Aprianta, "Implementation of inverse kinematics in design of six-degree of freedoms platform for hardware in the loop simulation on quadcopter drones," in *2021 3rd International Symposium on Material and Electrical Engineering Conference (ISMEE),* Bandung, Indonesia: IEEE, Nov., pp. 148–153, 2021.

[14] N. Lilansa, Y. Rajib, and J. A. Mawardi, "Interface for quadcopter drone physical model hardware in the loop (HIL)," in *2021 3rd International Symposium on Material and Electrical Engineering Conference (ISMEE),* Bandung, Indonesia: IEEE, Nov., pp. 268–271, 2021.

[15] O. L. Olsen, "On the use of hardware-in-the-loop for teaching automation engineering," *2019 IEEE Global Engineering Education Conference (EDUCON)*, Dubai, United Arab Emirates, pp. 1308-1315, 2019.

[16] C. Moon, "Design and implementation of hardware-in-the-loop simulation environment using system identification method for independent rear wheel steering system," *Machines*, vol. 11, no. 11:996, 2023.

[17] M. Z. Romdlony and F. Irsyadi, "Hardware-in-the-loop simulation of DC motor as an instructional media for control system design and testing," *J. Mechatron. Electr. Power Veh. Technol.*, vol. 12, no. 2, pp. 81–86, Dec. 2021.

[18] M. Goubej and M. Langmajer, "Experience with use of HIL simulators in control engineering course," *IFAC-PapersOnLine*, vol. 53, issue 2, 2020.

[19] I. Tejado, J. Serrano, E. Perez, D. Torres, and B. M. Vinagre, "Low-cost hardware-in-the-loop testbed of a mobile robot to support learning in automatic control and robotics," *IFAC-PapersOnLine*, vol. 49, issue 6, pp. 242 - 247, 2016.

[20] Y. Martinez-Armero, S. Lopez-Blandon, and E. Giraldo, "low-cost arduino-based hardware-in-the-loop platform for simulation and control of dynamic systems," *International Journal Of Computer Science*, vol. 50, issue 4, 2023.

[21] W. Jiang, L. Sun, Y. Chen, H. Ma, and S. Hashimoto, "A hardware-in-the-loop-on-chip development system for teaching and development of dynamic systems," *Electronics*, vol. 10, no. 7, p. 801, Mar. 2021.

[22] X. Zhang, H. Kong, and H. Wang, "A composite control scheme for automotive steer-by-wire system," in *Proceedings of 2014 International Conference on Modelling, Identification & Control*, Melbourne, Australia: IEEE, Dec., pp. 237–242, 2014.

[23] H. Gassmann, Theorie der Regelungstechnik. Verlag Harri Deutsch, 1998.